Reaching the quantum noise limit in a high-sensitivity cold-atom inertial sensor

Florence Yver-Leduc, Patrick Cheinet, Jérôme Fils, André Clairon, Noël Dimarcq, David Holleville, Philippe Bouyer, Arnaud Landragin

Reaching the quantum noise limit in a high-sensitivity cold-atom inertial sensor

Florence Yver-Leduc[1], Patrick Cheinet[1], Jérôme Fils[1], André Clairon[1], Noël Dimarcq[1], David Holleville[1], Philippe Bouyer[2] and Arnaud Landragin[1]

[1]BNM-SYRTE, UMR 8630, Observatoire de Paris, 61 avenue de l'Observatoire, 75014 Paris, France

[2]Laboratoire Charles Fabry, UMR 8501, Centre Scientifique d'Orsay, Bät 503, BP 147, 91403 Orsay, France

In our high-precision atom interferometer, the measured atomic phase shift is sensitive to rotations and accelerations of the apparatus, and also to phase fluctuations of the Raman lasers. In this paper we study two principal noise sources affecting the atomic phase shift, induced by optical phase noise and vibrations of the setup. Phase noise is reduced by carrying out a phase lock of the Raman lasers after the amplification stages. We also present a new scheme to reduce noise due to accelerations by using a feed-forward on the phase of the Raman beams. With these methods, it should be possible to reach the range of the atomic quantum projection noise limit, which is about 1mradrmsfor our experiment, i.e. 30 nrad s^{-1} $Hz^{-1/2}$ for a rotation measurement.

Keywords: Atom interferometer, Raman transitions, laser phase lock, phase noise in optical fibres, acceleration compensation in precision measurements

1. Introduction

Recent progress in atom interferometry [1] enables the development of new inertial sensors, using the potential of matter-waves to lead to high-precision detectors. Since the first atom interferometer showing a phase shift owing to rotation in 1991 [2], several gyroscopes have been developed and their sensitivities are already similar to those obtained with the best optical gyroscopes [3]. The first high-sensitivity measurement of the local acceleration of gravity based on atom interferometry was achieved the same year, and has been strongly improved since [4].

In the last decade, the laser cooling techniques have been considerably improved and developed for metrological applications, as exemplified in the field of atomic clocks [5]. For inertial sensors based on de Broglie waves, they lead to drastic improvements in stability and sensitivity, while enabling a reduction of the dimensions of the apparatus.

High-sensitivity inertial sensors with good long-term stability have applications in various domains: gravimetry and gradiometry, inertial navigation, geophysics, measurements of fundamental constants [6] and tests of general relativity, like the equivalence principle and the Lense–Thirring effect [7].

2. Description of our apparatus

The design of our apparatus has been guided by two goals: long-term stability and compactness. The expected sensitivity is 30 nrad s^{-1} $Hz^{-1/2}$ as a rate-gyroscope and 4×10^{-8} m s^{-2} $Hz^{-1/2}$ as an accelerometer, when about 10^6 atoms are detected at the output of the interferometer. This corresponds to a signal-to-noise ratio of 1000, so that the atomic quantum projection noise limit is 1 mrad rms.

A scheme of the setup is shown in figure 1. The atomic sources are caesium atoms cooled in a magneto-optical trap to a few microkelvin. Then, the atoms are launched by a moving molasses technique at 2.4 m s^{-1} with a repetition rate of 2 Hz. This value corresponds to the first characteristic frequency of the instrument, leading to a pass band of the

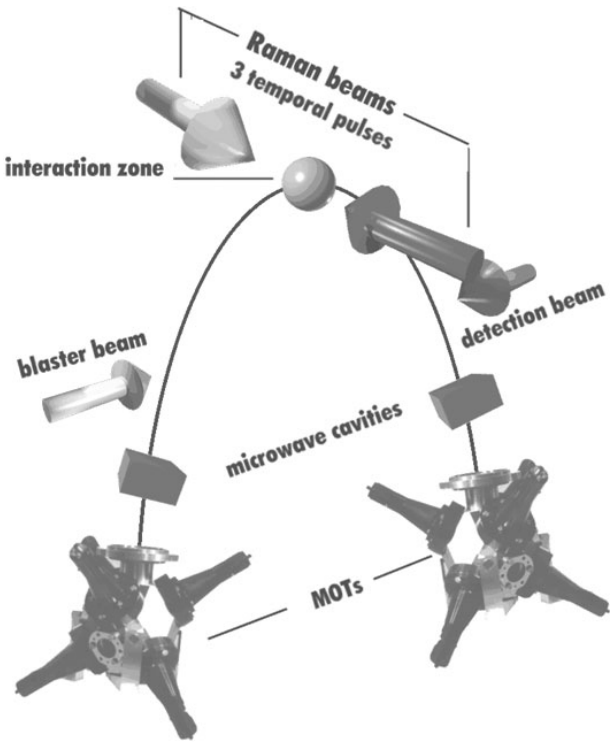

Figure 1. Principle of our cold atom inertial sensor. It uses two atomic sources launched in opposite trajectories and sharing the same Raman lasers. Horizontal velocity: 0.3 m s^{-1}.

interferometer of about 1 Hz. The atoms are prepared in the ($6S_{1/2}$, $F = 3, m_F = 0$) state by using microwave and optical pulses, and then reach the interferometer zone. The duration of one measurement in this zone is $2T \leqslant 100$ ms, which defines the second characteristic frequency of the instrument.

The interferometer configuration is similar to an optical Mach–Zehnder interferometer, and uses a $\pi/2{-}\pi{-}\pi/2$ sequence of counterpropagating laser pulses to induce stimulated Raman transitions [8] and coherently manipulate the atomic wavepackets (splitting, deviation and recombination). At the output of the interferometer, we measure the population of both hyperfine states ($6S_{1/2}$, $F = 3, m_F = 0$) and ($6S_{1/2}$, $F = 4, m_F = 0$) by laser-induced fluorescence and calculate the transition probability P between the two states.

The transition probability P is a function (1) of accelerations in the direction of the Raman laser beams, (2) of the rotation rate around the axis normal to the oriented area enclosed between the two arms of the interferometer, and (3) of fluctuations of the phase difference between the Raman lasers [9]. This last point will be further discussed in section 3. The phase shifts induced on the atomic wave phase are respectively named $\Delta\Phi_{acc}$, $\Delta\Phi_{rot}$ and $\Delta\Phi_{laser}$. The transition probability induced by the Raman sequence can be written as

$$P = \tfrac{1}{2}[1 + C\cos(\Delta\Phi_{acc} + \Delta\Phi_{rot} + \Delta\Phi_{laser})] \qquad (1)$$

where C is the contrast of the atomic fringes.

In order to distinguish between atomic phase shifts induced by rotation and acceleration, the experiment uses two counterpropagating atomic clouds diffracted by the same Raman pulses. The phase shifts measured by the two interferometers are then opposite for rotations, while they are identical for both accelerations and laser fluctuations. We thus discriminate between acceleration and rotation by adding or subtracting the phase shifts extracted from the two atomic clouds signals, as already demonstrated in [10].

Atom interferometry using either time domain (pulsed laser beams) [11] or space domain (focussed continuous laser beams) [12] can be built. The interferometer phase shifts induced by rotation and acceleration are

$$\Delta\Phi_{rot} = 2k_{eff}\Omega V T^2 \qquad (2)$$

$$\Delta\Phi_{acc} = k_{eff} a T^2 \qquad (3)$$

for an interferometer operating in the time domain, and

$$\Delta\Phi_{rot} = 2k_{eff}\Omega\frac{L^2}{V} \qquad (4)$$

$$\Delta\Phi_{acc} = k_{eff} a\frac{L^2}{V^2} \qquad (5)$$

in the space domain. $k_{eff} \cong 2k_{laser}$ represents the effective wavevector of the Raman laser pair, Ω is the rotation rate, and a the acceleration. In normal operation, V is the horizontal projection of the atomic mean velocity. T corresponds to the time between two successive Raman pulses and L is the spatial distance between two successive Raman beams.

In the time domain, the parameter determining the scaling factors is the time T between two successive interactions, whereas the important parameter in the space domain is the distance L between them.

A precise measurement requires a good definition of the scaling factor. Compared to thermal atomic beams, cold atom sources enable a smaller velocity dispersion of the atomic cloud and a better defined velocity by the use of the moving molasses technique. This leads to a better definition of the rotation scaling factor. Also, acceleration rejection by the use of two counterpropagating atomic clouds is more efficient in the time domain, as the velocity of the atoms does not appear in the scaling factor, which is thus better defined. For these reasons we have chosen to work with cold atoms and in the time domain.

Time intervals can be measured with a very high precision: in our apparatus, Raman pulses are generated by an acousto-optic modulator (AOM) with less than 100 ns rise time. Moreover, when using cold atoms launched by a moving molasses, the velocity of the atoms is very well known and stable: we can reach a stability of 10^{-4} m s^{-1} or better from shot to shot. The scaling factor of the gyroscope is then very well defined, and we can expect to know the rotation scaling factor with a relative uncertainty of 4×10^{-5} or better in one cycle. In the case of the Earth rotation rate measurement, this ensures an uncertainty below 3 nrad s^{-1} per shot, which is ten times lower than the short-term interferometer sensitivity.

Furthermore, the three laser pulses are generated by switching on and off three times the same pair of large Raman laser beams. The rotation noise induced in space domain gyroscopes by misalignments of the Raman laser pairs between each other is thus strongly reduced in our case.

However, our setup is also sensitive to temporal fluctuations of the Raman phase difference, which can lead to a degradation of the signal-to-noise ratio.

3. Influence of phase noises on rotation and acceleration measurements

The atomic phase shift measured at the output of the interferometer is a function of the phase difference between the two counterpropagating Raman lasers [13]:

$$\Delta\Phi_{laser} = \Phi_1(t) - 2\Phi_2(t+T) + \Phi_3(t+2T) \qquad (6)$$

where $\Phi_i(t)$ represents the phase difference between the two Raman lasers during the ith pulse. This phase is considered at the location of the centre of the atomic wavepacket [14]. This means that the atomic phase shift measured is also sensitive to any fluctuations of the phase difference between the Raman pulses. As laser phase noise induces identical phase shifts for both atomic clouds, it is seen as acceleration by the interferometer.

For an acceleration measurement, phase noise on the Raman phase difference and vibrations of the setup have to be minimized so that their contributions to the atomic phase noise remain below the 1 mrad rms interferometer noise.

For a rotation measurement, laser phase noise is rejected by the use of two counterpropagating atomic clouds. However, the phase shifts induced by these perturbations must remain negligible compared with 2π, in order to avoid any ambiguity on the fringe number. Moreover, to simplify the extraction of rotation and acceleration phase shifts from the experimental signals, the interferometer's phase fluctuations and vibrations should be reduced to less than 0.1 rad rms, which allows a linearization of equation (1) near the operating point.

In our setup, we have implemented a phase lock scheme that enables a reduction of the phase noise induced by the semiconductor (SC) amplifiers. In addition to a passive isolation from the vibrations, we also show here the possibility to implement a feed-forward compensation of the effect of vibrations by directly acting on the phase of the Raman beams.

4. Measurement and rejection of the phase noise of the Raman beams

The difference between the two Raman laser frequencies must be stabilized at 9.19 GHz to be tuned to the clock transition frequency of the caesium atoms. This stabilization is also crucial to prevent any degradation of the signal-to-noise ratio in the interferometer.

Several noise sources could spoil the Raman phase difference: internal noise of the microwave generator, optical amplification by slave lasers, independent propagation of the beams through air and various optical elements (AOM, polarization maintaining fibre). In this study, we will focus on optical phase noise sources, such as optical amplification and propagation in the polarization maintaining fibre, and on their contributions to the interferometer noise.

In order to deduce the contribution of the optical phase noise to the noise degrading the atomic phase shift, the measured phase noise spectra have to be weighted by the interferometer transfer function. As shown in equation (6), the atomic phase shift measurement consists in reading the Raman phase difference at three times $t = 0, T, 2T$, because of the $\pi/2-\pi-\pi/2$ configuration. We calculate the transfer function by expressing the atomic phase shift as a function of fluctuations of the phase difference $\Phi_i(t)$ between the two Raman lasers during the ith pulse.

We first suppose that the three laser pulses have an infinitely short duration. When expressing the Fourier transform of the laser phase fluctuation, with amplitude Φ_f and arbitrary phase φ_f at frequency f, each $\Phi_i(t)$ corresponding to the phase difference between the two Raman lasers during the ith pulse can be written as

$$\Phi_i(t) = \int_f \Phi_f \cos\,(2\pi f t + \varphi_f)\,\mathrm{d}f. \qquad (7)$$

Calculated from equation (6), the atomic phase shift induced by the laser phase fluctuation component at frequency f is thus

$$\Delta\Phi_{laser}(f) = -4\Phi_f \sin^2(\pi f T)\cos(2\pi f T + \varphi_f). \qquad (8)$$

A quadratic average of equation (8) on the arbitrary phase φ_f gives the contribution of the laser phase fluctuation to the atomic phase shift at frequency f:

$$\sqrt{\langle \Delta\Phi^2_{laser}(f)\rangle_{\varphi_f}} = 2\sqrt{2}\Phi_f \sin^2(\pi f T). \qquad (9)$$

The rms atomic phase shift due to a laser phase fluctuation at frequency f is thus obtained by multiplying the amplitude Φ_f of the fluctuation by a transfer function defined by a square sine function of the frequency f. This implies that the interferometer transfer function cancels at frequency multiples of $1/T$ and expresses the fact that the atomic phase shift measurement results in a sampled measurement of the rotation rate or the acceleration [4].

Furthermore, the study of the real case of square Raman pulses with a finite duration τ induces a well-known first-order low-pass filter in the transfer function of the interferometer, with a cut-off frequency $f_c = 1/2\tau$. From equation (9), the transfer function of the interferometer can be written as

$$|H(f)|^2 = \frac{8\sin^4(\pi f T)}{1 + (\frac{f}{f_c})^2} \qquad (10)$$

where T is the time interval between two consecutive Raman pulses, and f_c the cut-off frequency of the low-pass filter due to the pulses' finite duration τ ($\tau = 30\ \mu$s in our experimental case).

Each measured phase noise spectrum has thus to be weighted by this transfer function in order to evaluate its contribution to the noise degrading the atomic phase shift.

Phase noise measurements due to the optical amplification and to the propagation in the fibre are detailed after a short description of the optical bench generating the Raman laser beams.

The Raman laser beams are generated with two extended cavity laser diodes (ECLD) emitting at 852 nm. ECLD outputs are amplified to get the optical power needed for about 30 μs Raman pulses (figure 2). Therefore we use a slave laser diode (SD) for one path, from which we get 200 mW. On the other path, a tapered SC amplifier increases the laser power up to 500 mW. After superimposition in a polarization beam splitting cube, both beams are deflected by an AOM used as an optical switch to generate the three pulses. They are then injected with

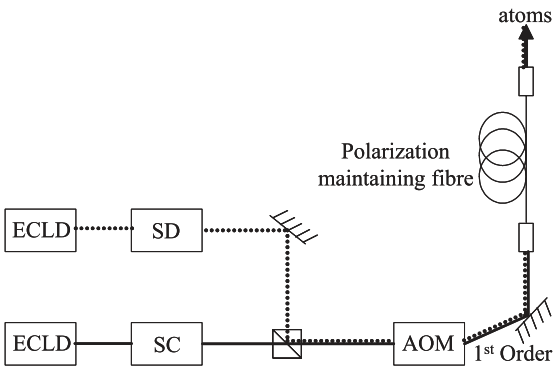

Figure 2. Principle of generation of the Raman laser beams. The laser frequency difference is 9.19 GHz and the AOM is used only as a switch of the Raman beams.

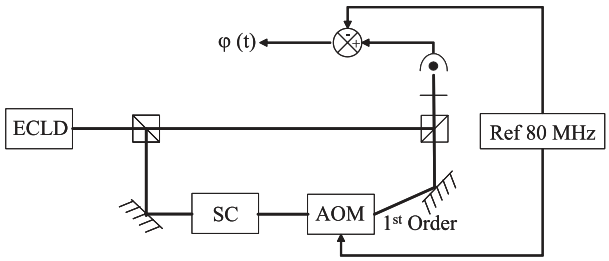

Figure 3. Scheme of the experiment used to measure the phase noise generated in the optical amplification path using the SC amplifier.

crossed polarizations into the two proper axes of a polarization maintaining fibre and propagate towards the interaction zone with the atoms.

The first step is to measure the phase noise induced by one of the two amplification stages, realized with the SC amplifier. The injection of the slave diode is supposed to add a similar phase noise. A photodiode detects the beat-note between the ECLD and the amplified laser beam, frequency shifted by 80 MHz using an AOM (figure 3). Phase noise is measured by mixing the photodiode output with a reference signal at 80 MHz.

The power spectral density (PSD) of the phase noise spoiling this beat-note is shown in figure 4. Low-frequency noise up to 3 kHz is due to temperature fluctuations on the optical bench and in the SC amplifier, and to mechanical vibrations. At higher frequencies, phase noise sources are mostly electrical and result in high narrow peaks of noise.

After weighting this spectrum by the interferometer transfer function to phase fluctuations described in equation (10), we estimate the atomic phase noise induced by the SC amplifier at the level of 180 mrad rms. This value greatly exceeds the limit of 1 mrad rms set by the expected signal-to-noise ratio of 1000.

We have to implement a method to imprint the phase quality of the microwave generator on the Raman phase difference. Usually, this Raman laser frequency stabilization is realized by phase locking one ECLD on the other [15]. But, doing so, the phase noise induced by the amplification stages is not compensated for, and degrades the phase difference between the laser beams at the level previously measured. That is the reason why we chose to phase lock the Raman laser beams after the optical amplification stages. With this method,

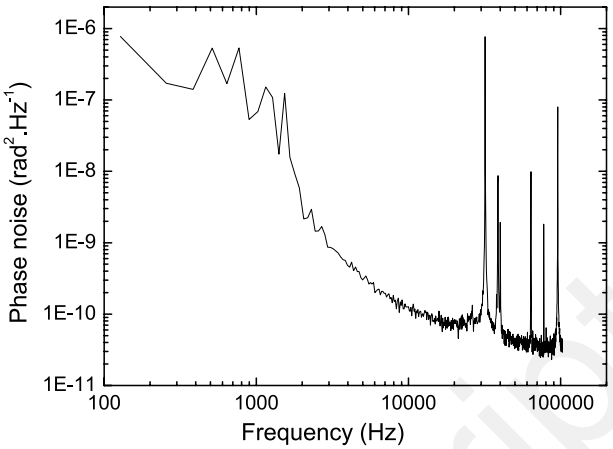

Figure 4. PSD measured in the experiment described in figure 3. The phase noise is mostly due to the SC amplifier and optical path fluctuations.

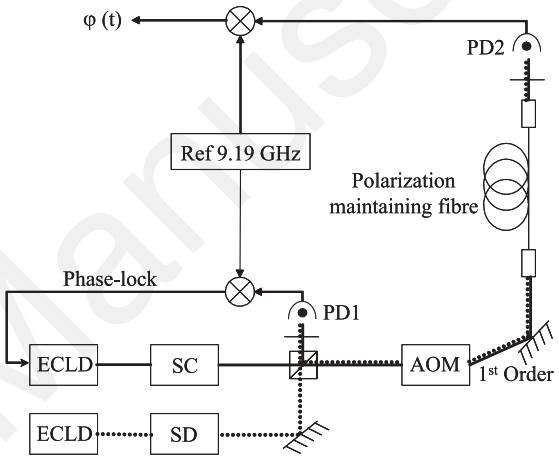

Figure 5. Principle of measurement of the residual phase noise between the two phase-locked Raman beams, directly imprinted on the atomic wave phase.

the loop delay is certainly increased, but all optical phase shifts introduced while the Raman beams do not copropagate are strongly reduced.

One could propose that the phase noise induced by the polarization maintaining fibre can also be rejected with a phase lock after the fibre. But, as Raman lasers are pulsed by the AOM, it is impossible to make any continuous servo-control including this AOM in the loop. The only way to servo-control the phase shift after the fibre is to use an external continuous laser, far detuned from the atomic transitions and copropagating in the optical fibre. For reasons of simplicity and easy implementation, the Raman laser beams are phase locked just before the AOM. Residual noise spoiling the phase difference between the phase-locked lasers is measured after propagation in the polarization maintaining fibre, in order to control whether this method is sufficient to preserve a high signal-to-noise ratio.

The phase difference between the two amplified laser beams is phase locked at the superimposition point by carrying out a beat-note between the laser beams on a Hamamatsu ultrafast photoconductor G4176, named PD1 (figure 5). The amplified beat-note is mixed with a reference signal at

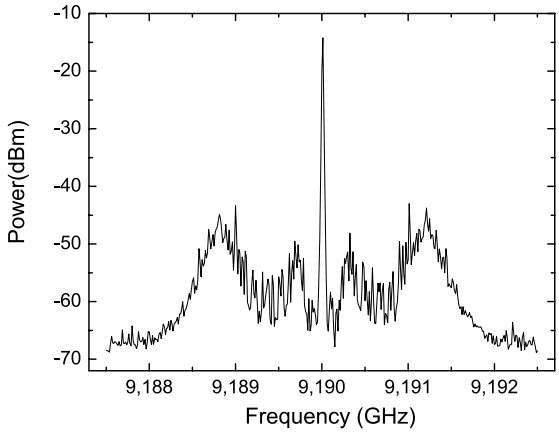

Figure 6. Beat-note detected on the photoconductor PD1, with a resolution bandwidth of 10 kHz. The central peak contains about 90% of the total power.

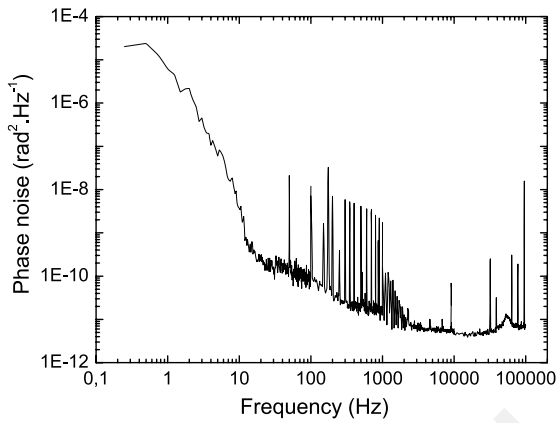

Figure 7. PSD of the phase noise measured on PD2 after the phase lock and propagation in the fibre. This Raman phase noise is directly seen by the atoms.

9.19 GHz. The error signal is then used to generate a correction signal fed back to the ECLD current and piezo-electric transductor (PZT).

Figure 6 shows the beat-note measured by a spectrum analyser with a resolution bandwidth of 10 kHz. We observe a lock bandwidth of 1.2 MHz. This is enough to reduce the phase noise of the Raman beams to the phase noise level of the microwave generator.

In figure 7 is shown the residual phase noise after propagation in a 3 m long optical fibre, and table 1 gives the induced phase noise in the atom interferometer after weighting by $H(f)$ (see equation (10)), for each frequency decade.

We can see a high phase noise at low frequencies up to 10 Hz. This phase noise is due to temperature fluctuations in the polarization maintaining fibre. For comparison, we measured the phase noise induced by propagation without any fibre, which showed a much lower contribution to the atomic phase noise in this decade (0.38 mrad rms compared to 1.01 mrad rms).

At Fourier frequencies from 100 Hz to 1 kHz, we measure many peaks at harmonic frequencies of 50 Hz. Their contribution to the atomic phase noise is significant (0.49 mrad rms) but does not represent the principal noise source. Moreover, they could come from electrical artefacts and their existence on the Raman phase difference is not certain. This means that the contribution of the frequency band from 100 Hz to 1 kHz to the atomic phase noise is probably lower than what we measured.

Table 1. Contribution of the Raman phase noise in each frequency decade calculated from the PSD (figure 7) weighted by the interferometer transfer function $H(f)$.

Frequency band	Atomic phase noise (mrad rms)
0–10 Hz	1.01
10– 100 Hz	0.37
100 Hz–1 kHz	0.87
1 kHz–10 kHz	0.48
10 kHz–100 kHz	0.37
Total	1.51

At frequencies higher than 1 kHz, the PSD reaches the noise level of the measurement setup.

Thus, a direct phase lock of optical amplified lasers enables a rejection of the major part of the phase noise induced by the amplification stages and non-counterpropagating paths. With this method, the contribution of the Raman lasers' phase noise falls down to the level of 1.5 mrad rms.

The optical fibre is the most important source of noise on the Raman laser phase difference. With a better control of the fibre temperature, we expect to reduce the interferometer phase noise to the range of 1.2 mrad rms.

5. Acceleration compensation

Because of an aliasing effect due to our sampling frequency of 2 Hz, the high-frequency part of the acceleration noise is transferred to the low frequencies (lower than 1 Hz) and can degrade the signal-to-noise ratio of the interferometer. In order to evaluate the effect of vibrations on the interferometer, we measured the acceleration noise and deduced its contribution to the interferometer phase shift by weighting it by equation (10). Because the interferometer signal depends only on the difference of position (or phase) between the three pulses (see equation (6)), the accelerometer signal has to be converted in a position (or phase) signal. This means that it has to be integrated in the frequency band from 0.1 to 200 Hz. Vibrations of the lab floor have been measured with an accelerometer (IMI model 626A04) and would contribute to the interferometer phase noise at the level of 1 rad rms. This value is too high compared with the limits of 1 mrad rms and 0.1 rad rms required respectively for acceleration and rotation measurements.

Two methods can be implemented to reduce vibrations of the setup: putting it on an isolation platform or compensating for vibrations actively. We installed our interferometer on an optimized NanoK isolation platform. This enabled us to reduce vibrations so that their contribution to the interferometer phase noise is estimated at about 0.1 rad rms. This method, alone, is not sufficient to reach the interferometer sensitivity. Moreover, the platform could lead to additional rotation noise [4]. For these reasons, we have tested a new scheme to reduce the effect of vibrations by using a feed-forward on the phase of the Raman beams. If the method is efficient and robust enough, it will be possible to avoid using any vibration isolation platform.

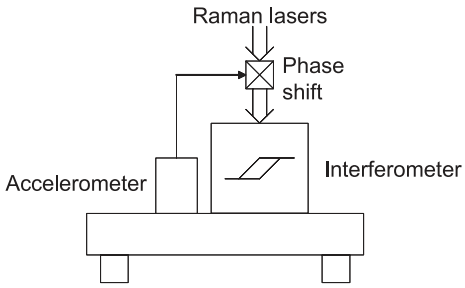

Figure 8. Principle of setup for acceleration compensation on the inertial sensor. The accelerometer signal is used to generate a correction signal on the Raman phase, which cancels the phase shift induced by vibrations.

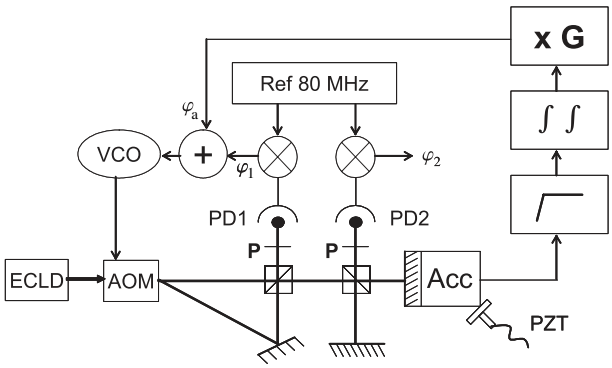

Figure 9. Auxiliary experiment testing the acceleration rejection. The accelerometer signal is used as a feed-forward correction signal and is added into the Raman phase lock loop.

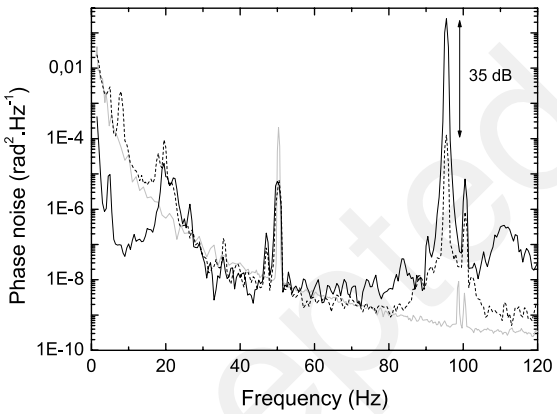

Figure 10. PSD of the phase noise measured on PD2 (figure 9). Solid curve: without rejection. Dashed curve: with rejection. Grey curve: accelerometer's internal noise.

The basic principle of the method is schematized in figure 8. A low-noise sensor is rigidly fixed on the table supporting the interferometer. This sensor provides an acceleration signal at high frequencies used in the feed-forward compensation on the phase of the Raman beams. After the two integrations and proper adjustment of the gain, it is applied to the phase lock setup of the Raman beams. This adjustment can be performed by minimizing the interferometer noise. By doing so, we have the advantage of the high sensitivity of mechanical accelerometers at high frequencies and the stability of atomic interferometers at low frequencies and continuous accelerations.

In order to test this method, we built the auxiliary experiment schematized in figure 9. The first step is to implement a setup similar to the original optical bench. The two laser beams representing the Raman lasers come from the same ECLD diffracted in zero and first orders of an AOM, fed with a voltage-controlled oscillator (VCO). The two laser beams are then recombined in a polarization beam splitting cube.

At one output of the cube, a first photodiode PD1 measures the beat-note between the two beams. This signal is mixed with an 80 MHz reference signal to obtain the phase error signal φ_1 used to drive the VCO feeding the AOM. In this way, we servo-lock the phase difference between the two beams at the location of the photodiode, as it is done in the original setup.

At the second output, the beams are separated again into a Michelson interferometer and we simulate vibrations of the setup by moving one mirror with a PZT. A second photodiode PD2 is placed at the output of the interferometer to measure the optical phase shift φ_2 that would be imprinted on the atomic wave phase.

Our method to compensate for this phase shift consists in measuring the mirror's vibrations with an accelerometer to generate a correction signal. For this study, we use an accelerometer working in the frequency range from 0.1 to 200 Hz. In order to suppress low frequencies below 0.1 Hz which lead to a drift of the correction signal, we use a high-pass filter with a cut-off frequency of 0.16 Hz. The signal has to be integrated twice and scaled in order to be compared with φ_2. The integration used a second-order low-pass filter with a cut-off frequency of 3 Hz. Finally, this correction signal, named φ_a, is added to the phase error signal φ_1 of the servo-loop. When the compensation is perfectly adjusted, no modulation induced by the PZT should appear on φ_2. The scaling factor G is chosen experimentally to minimize the modulation of φ_2.

We show in figure 10 the PSD of the phase noise measured on PD2 for an excitation frequency of 95 Hz, with and without feed-forward compensation, and the equivalent accelerometer's internal noise previously measured.

Any active rejection will add the noise of its reference. Here, the feed-forward compensation adds the accelerometer's noise to the final measured phase noise. One can notice that, at low frequency (below 60 Hz), the accelerometer's noise is at the level of or higher than the vibration noise. This leads to an increased noise level for frequencies lower than 20 Hz in this case. Wherever the accelerometer's noise is low enough, we observe a decrease of the noise level and we reach a 35 dB rejection efficiency for the frequency modulation of the PZT at 95 Hz.

To fully characterize the rejection process, the last step is to study the efficiency of the vibration compensation as a function of the modulation frequency. To do so, we use a PZT modulation amplitude high enough to be only partially rejected, so that the rejection process is not limited by the accelerometer's noise. We found a strong dependence on the modulation frequency. In order to better understand this result, we modelled the rejection efficiency, taking into account the processing of the acceleration signal before its addition in the servo-loop.

For low frequencies, the phase shift introduced by the high-pass filters and integration device prevents an exact cancellation. This will reduce the rejection efficiency. For

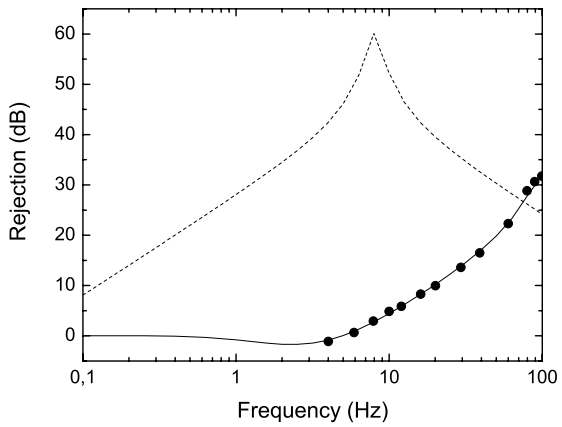

Figure 11. Phase noise rejection of the modulation induced by the PZT. Black dots: experimental result. Solid curve: simulated rejection in the actual experimental conditions. Dashed curve: calculated rejection that could be obtained by using a better accelerometer with a lower noise level and a lower working frequency (0.01 Hz cut-off frequency).

the best rejection efficiency, the scaling factor error will limit the rejection.

Finally, for the highest frequencies, the accelerometer's sensitivity presents a mechanical resonance around 2 kHz. This will induce a decrease of the rejection efficiency.

We can see in figure 11 that the simulation is in good agreement with the experimental results. This means that the rejection measured here is limited by the analogical processing of the signal.

We plan to replace the accelerometer by a seismometer working in the 0.01–50 Hz frequency range, which presents a lower noise level (Guralp CMG-T40). This will allow us to reduce the cut-off frequencies on the analogical filters, in order to optimize the rejection. We plotted also in figure 11 with a dashed curve the case with cut-off frequencies of 0.01 Hz, with a scaling error of 1:1000. This will lead at least to a 25 dB rejection from 1 to 100 Hz. We could further improve this result by using a numerical filtering instead of an analogical one. This would enable the use of the optimum filter taking into account the real transfer function of the setup.

Traditional criticisms made against feed-forward compensation schemes concern the difficulties due to the need for a very good knowledge of the scaling factors. They do not really apply here for at least three reasons: first, we only need to reduce the interferometer phase noise induced by high-frequency noise aliased to low frequency. Second, the compensation is not totally an open-loop configuration; a numerical minimization of the interferometer noise allows at least for gain adjustment of the vibration compensation in the long term. Third, we do not suspect the mechanical transfer function to vary significantly during the course of a measurement.

6. Conclusions

In this paper we have demonstrated our ability to reduce two principal noise sources in the atom interferometer. A phase lock after the amplification stages reduces the phase noise on the Raman phase difference. The residual noise contributes to the atomic phase noise at the level of 1.5 mrad rms.

A preliminary test of acceleration compensation by acting on the optical phase has been validated. The method enables us to reach a 35 dB rejection, and this value can be easily improved by using a seismometer with better low-frequency internal noise. This should allow us to operate the inertial sensor on the ground and perhaps to free the setup from potential rotation noise added by the isolation platform.

More work is necessary to fully demonstrate the efficiency of this feed-forward vibration compensation. However, it looks very promising and its implementation is much easier than the traditional method used for active vibration isolation. A generalization to three dimensions is possible, and it could also be applied in other high-precision measurements, particularly for vibration compensation of lasers stabilized in supercavities.

Thus, we expect that these two main noise sources can be reduced to the intrinsic limit of the interferometer sensitivity. The remaining main noise source is due to wavefront distortions of the Raman lasers. This can lead to a systematic error if the two atomic trajectories do not perfectly overlap [16].

Acknowledgments

The authors would like to thank CNRS, BNM, DGA, SAGEM and CNES for supporting this work. We would also like to thank the electronic staff of SYRTE for their help and advice.

References

[1] Berman P R (ed) 1997 *Atom Interferometry* (London: Academic)
[2] Riehle F, Kister Th, Witte A, Helmcke J and Bordé Ch J 1991 *Phys. Rev. Lett.* **67** 177
[3] Gustavson T L, Landragin A and Kasevich M 2000 *Class. Quantum Grav.* **17** 1
[4] Peters A, Chung K Y and Chu S 2001 *Metrologia* **38** 25
[5] Clairon A, Laurent Ph, Santarelli G, Ghezali S, Lea S N and Bahoura M 1995 *IEEE Trans. Instrum. Meas.* **44** 128
[6] Wicht A, Hensley J M, Sarajlic E and Chu S 2001 *Proc. 6th Symp. on Frequency Standards and Metrology* ed P Gill (Singapore: World Scientific) p 193
[7] *ESA Assessment Study Report* 2000 ESA-SCI 10
[8] Bordé Ch J 1991 *Laser Spectroscopy* vol 10, ed M Ducloy, E Giacobino and G Camy (Singapore: World Scientific) p 239
[9] Storey P and Cohen-Tannoudji C 1994 *J. Physique* II **4** 1999–2027
[10] Gustavson T L, Bouyer P and Kasevich M 1998 *Proc. SPIE* **3270** 62
[11] Sterr U, Sengstock K, Ertmer W, Riehle F and Helmcke J 1997 *Atom Interferometry* ed P R Berman (London: Academic)
[12] Udem Th, Diddams S A, Vogel K R, Oates C W, Curtis E A, Lee W D, Itano W M, Drullinger R E, Bergquist J C and Hollberg L 2001 *Phys. Rev. Lett.* **86** 4996
[13] Kasevich M and Chu S 1992 *Appl. Phys.* B **54** 321
[14] Antoine C and Bordé Ch J 2002 *Phys. Lett.* A **306** 277
[15] Santarelli G, Clairon A, Lea S N and Tino G 1994 *Opt. Commun.* **104** 339
[16] Landragin A, Fils J, Yver F, Holleville D, Dimarcq N and Clairon A 2001 *Proc. 6th Symp. on Frequency Standards and Metrology* ed P Gill (Singapore: World Scientific) p 532